



## Metamaterial inspired contactless angular displacement sensor with wide dynamic range and bandwidth

Nilesh Kumar Tiwari<sup>(1)</sup>, Surya Prakash Singh<sup>(1),(2)</sup>, M. Jaleel Akhtar<sup>(1)</sup>

(1) Department of Electrical Engineering, Indian Institute of Technology Kanpur, Kanpur-208016, UP, India

(2) Department of Electronics and Telecommunication Engineering, IIIT Bhubaneswar, Bhubaneswar-751003, Odisha, India

### Abstract

A new design approach of microwave rotation sensor using separated ring of double split ring resonator (DSRR) is presented in this work. The proposed sensor provides the contactless determination of angular displacement by investigating the shift in resonant frequency. The novel design configuration helps to obtain the wide dynamic range, resolution, linearity and sensitivity. In this work two rings of DSRR has been separated vertically to attach them one at stator and other one at rotor to perform the contact less wide range rotation measurement using the asymmetry of rectangular SRR ring. Rotation of inner ring attached on the rotor results into change in its coupling with the outer ring present at the stator. This actually changes the overall capacitance of the sensing region thereby changing the resonant frequency of the sensor. The designed sensor dimensions are optimized in order to get the improved sensitivity and linearity in the wide dynamic range of 0 to 120°. Maximum achievable frequency shift using the proposed sensor is found to be nearly 19 MHz/°. Moreover, the designed sensor can cover the maximum angular displacement range of nearly 5 mm with 2 GHz bandwidth using only the single sensor arrangement, unlikely the multi cell SRR arrangement where the maximum displacement coverage is ~ 1mm with 0.5 GHz bandwidth.

### 1. Introduction

Resonant microwave sensor has been extensively used for various applications in the RF/Microwave frequency region during the last few decades [1]-[4]. Resonant microwave sensors based on the conventional metallic cavity structure generally possess the very high quality factor that helps to obtain the better accuracy in the extracted parameters [4]. However, in recent years the sensors have been mainly realized using the planar resonant structures such as ring resonator, substrate integrated cavity and metamaterial particle based sensors. Interdigital capacitor (IDC), split ring resonator (SRR) and complementary split ring resonator (CSRR) are the most widely used metamaterial particles used for range of microwave applications [1]-[3]. Design of planar sensor using the metamaterial particle can be considered as one of the important aspect of these structures [1]. The planar microwave sensor based on the metamaterial particle basically helps to localize the strong electric/magnetic field

in the electrically small region which facilitates the realization of compact sensor topology with excellent sensitivity and resolution. These unique features of the metamaterial particle loaded structures have been extensively exploited by various researchers to design the different kind of sensors for wide range of applications [1], [4]. Recently, metamaterial inspired sensors have been demonstrated to design the rotation sensor for investigation of the angular displacement and rotational velocity for various industrial applications ranging from antenna industry, steel industry to the space industry [5]-[11]. For the antenna measurement using the linearly polarized antenna the proper alignment must be ensured to mitigate any error in the phase and gain measurement. Application of coplanar waveguide loaded especially designed SRR and electric LC resonator based structures for space application have been proposed [5]-[7] to measure the angular displacement where maximum considered displacement is 1mm with corresponding bandwidth of 600 MHz and dynamic range up to 90°. However, the parameter under consideration in these works is magnitude of transmission coefficient with sensitivity of 0.26 dB/°, which can easily be affected with the change in associated losses. Measurement of angular velocity using the circularly polarized antenna has presented using the detection of phase change that results into the more susceptibility toward noise [8]. In another work the horn shaped SRR resonator has been used to obtain the linearity in measurement for the small dynamic range of 8° [9]. The dynamic range and sensitivity has been improved up to 45° and 26.4 MHz/°, respectively using the metamaterial inspired structure [10]. The dynamic range of metamaterial inspired sensor is further increased up to 180° using the tapered U shaped resonator with overall bandwidth and resolution 350 MHz and 2MHz/° respectively [11].

From the above discussion it can be concluded that number of rotation sensors with their specific characteristic are available in literature but it is hard to realize the single sensor that can exhibit most of these features alone. Thus it is required to design the metamaterial inspired sensor in such a manner that the wide dynamic range, linearity and bandwidth can be realized using single sensor configuration, without any significant reduction in resolution.

Due to the above mentioned reason, a novel design configuration of metamaterial inspired angular displacement sensor is proposed in this paper. The inner ring of the DSRR is designed on the rotor section (target specimen), while its outer ring is designed at the stator (microstrip substrate). The induction of vertical air gap between these two rings actually helps to perform the contactless measurement of angular rotation/displacement. The mechanical change in displacement between these rings results into the change in effective coupling (dynamic behaviour) between them that eventually leads into change in the resonant frequency of the sensor. Moreover, the static coupling (between microstrip and outer ring of DSRR) can also affects the resonant frequency. Therefore, Numerical analysis of both the coupling mechanism, i.e., static and dynamic has been carried out using the different possible arrangements of the rings to understand the effect of coupling on the resonant frequency of the sensor.

## 2. Numerical design and analysis of the proposed rotation sensor

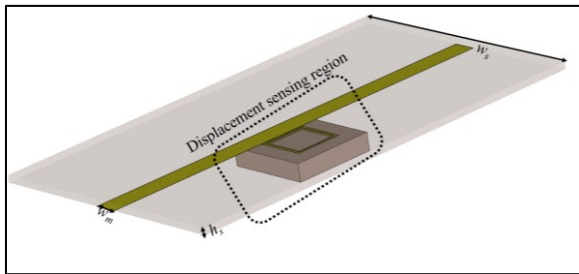


Figure 1. Numerical simulation model of the proposed sensor system with  $w_m=2.6$ ,  $h_s=0.8$  and  $w_s=30$  mm.

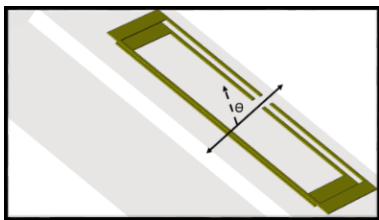


Figure 2. Vertically separated rings with the direction of rotation ( $\Theta$ )

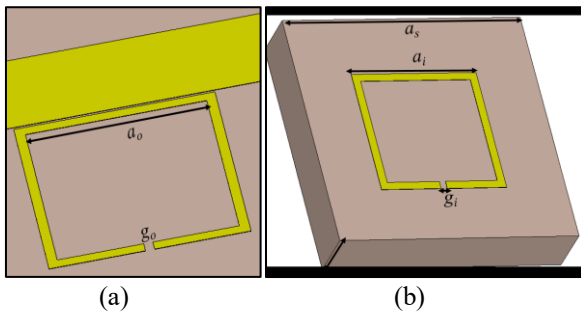


Figure 3. (a) Static part including microstrip coupled outer ring of DSRR. (b) Rotational part consist of inner ring of DSRR etched on the target specimen with  $a_o=5$  mm,  $g_o=g_i=0.25$  mm,  $a_s=9.55$  mm and  $a_i=4.4$  mm.

The numerical simulation model of the proposed rotation sensor designed using the CST-MWS as shown in Figure 1 and Figure 2 shows the rotation direction of rotational ring with their vertical interspacing to the static part. The design shown in Figure 1 contains the complete sensor system including the stationary microstrip coupled outer ring of SRR structure and vertically separated rotational part with 0.1 mm air gap. In the present case the inner ring of the DSRR designed on the target specimen act as the rotational system. Figure 3(a) and 3(b) helps to make clear interpretation about rotational part and stationary part with their specified dimensions. Here it is to be noted that the target under investigation (rotational part) rotate around the axis perpendicular to the plane of inner /outer ring of the sensing arrangement. The sensing mechanism of the proposed rotation sensor can be explained using the equivalent lumped equivalent circuit model of the proposed sensor as shown in Figure 4.

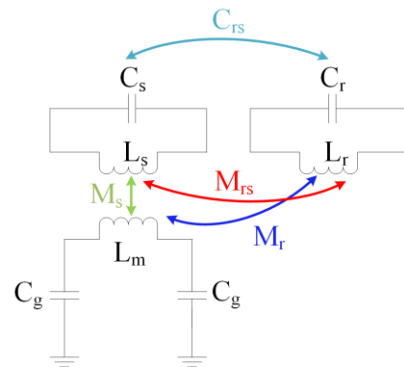


Figure 4. Equivalent circuit model of proposed rotation sensor. The  $C_s$ ,  $L_s$  and  $C_r$ ,  $L_r$  and  $C_g$ ,  $L_m$  represents the capacitance and inductance of stationary section, rotational section and the microstrip line.

From this figure it can be observed that the outer ring of the DSRR is magnetically coupled ( $M_s$ ) with the main microstrip line ( $L_m$ ,  $C_g$ ) whereas the inner ring of the DSRR is coupled with the outer DSRR ring and microstrip line with the variable coupling capacitance ( $C_{rs}$ ) and inductances ( $M_{rs}$ ,  $M_r$ ). The value of these variable coupling capacitance/inductance gets modified with the mechanical change in the angular rotation of the inner DSRR ring. This basically means that the overall capacitance/inductance of the sensing arrangement gets changed with the change in rotation of the rotational part, inner ring on the test specimen. Here, it is worth mentioning that apart from this dynamic coupling mechanism the static coupling mechanism also affects the resonant behaviour of the proposed sensing methodology. In the present situation, the coupling between the outer DSRR ring and the microstrip line can be termed as the static coupling coefficient while the mutual coupling between both the rings and coupling of inner rotational ring with the microstrip line is described as the dynamic coupling mechanism. Therefore, in next section, effect of both *viz.* dynamic and static coupling mechanism is studied in order to get the more insight about effective coupling arrangement for rotation sensor.

### 3. Numerical determination of rotation angle

Numerical determination of rotation angle is considered in this section by using different possible configuration of the static ring along with axial rotation of the rotational part. In first case, split of outer DSRR (static section) is oriented outward from microstrip line as shown in the Figure 5. After freezing the position of stationary arrangement, dynamic coupling arrangement has been varied by rotating the rotator ring (inner SRR) for wide range of angle. The rotation arrangement corresponding to three typical angles are shown in Figure 5. Here it is to note that the air gap between the rotor and static ring is kept fixed at 0.1mm. The change in resonant frequency corresponding to this arrangement is shown in Figure 6

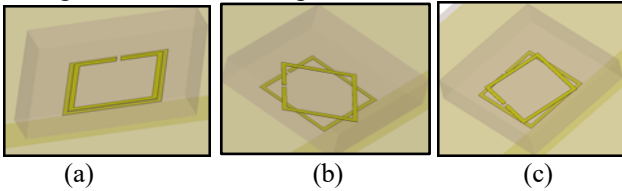


Figure 5. Configuration-I rotation sensor, (a)  $0^\circ$  rotation, (b)  $40^\circ$  rotation, (c)  $80^\circ$  rotation of the rotating SRR.

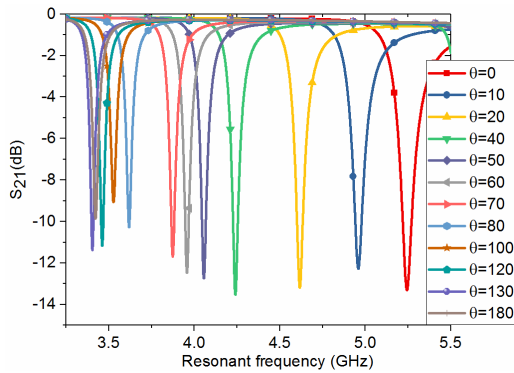


Figure 6. Plot of  $S_{21}$  for wide range of angular rotation.

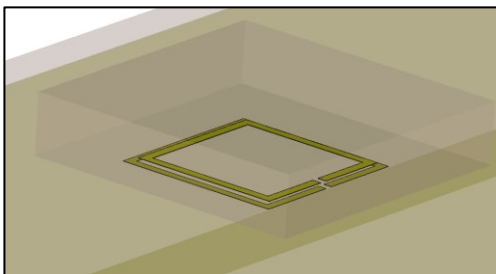


Figure 7. Configuration II sensor with  $0^\circ$  rotation angle

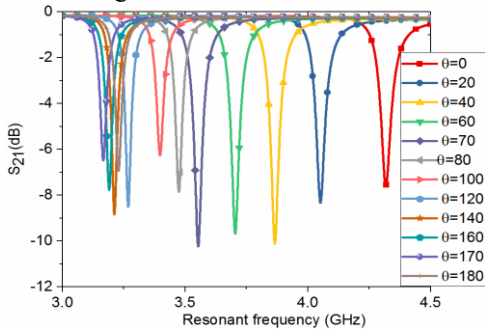


Figure 8. Plot of  $S_{21}$  for wide range of angular rotation.

From the figure, it can be noticed that the static resonant frequency without any rotation ( $\Theta=0^\circ$ ) is comes about 5.25 GHz. The dynamic range of this sensor configuration is  $120^\circ$  with almost linear behavior in this range. The next arrangement of rotational sensing is shown in Fig.7 where the slit of static ring is oriented along the feed line that results into static resonant frequency of 4.78 GHz, Fig.8. The obtained dynamic range is nearly  $160^\circ$  but the linearity region is limited to  $40^\circ$  which can be noticed from the plot shown in Figure 8. At last, the configuration shown in Figure 9 is used as sensing arrangement where the slit is oriented toward the feed line that produces the static resonant frequency of 4.3 GHz. The dynamic range of the proposed sensor is  $100^\circ$  with linearity range up to  $70^\circ$  which is quite clear from Figure 10. From the above three cases, it can be concluded that among all the configurations, the configuration-I possess better performance in term of linearity, bandwidth and sensitivity. It is worth mentioning here that the bandwidth coverage in this arrangement is nearly 2 GHz which is much higher than the earlier proposed operational bandwidth 0.35 GHz corresponding to  $180^\circ$  dynamic range [11]. The maximum achievable frequency shift/ $^\circ$  is 19 MHz/ $^\circ$  as compared to the earlier reported 2.5 MHz/ $^\circ$  in [11]. Moreover, the step size of  $10^\circ$  in present work produces the more shift in resonant frequency as compared to step size of  $20^\circ$  in earlier reported rotation sensor [5]. Thereafter, using the resonant frequency corresponding to this arrangement (configuration-I) for range of rotation angle is used to develop the graphical relationship with the rotation angle and or angular displacement as shown in Figure 11. From the graphical relation shown in this figure it can easily be observed that the proposed sensing arrangement produces the nearly linear relationship between the rotation angles and numerically generated resonant frequency. A typical calculation of the angular displacement shows that the proposed sensor can cover the angular displacement of  $\sim 4.8$  mm in the span of  $120^\circ$  rotation as compared to earlier reported value of 1 mm displacement.

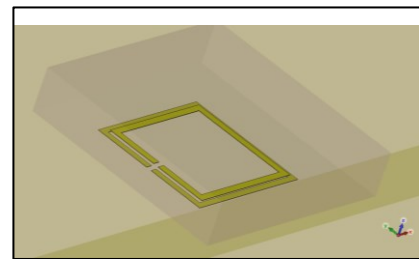


Figure 9. Configuration III sensor with  $0^\circ$  rotation angle

A comparative performance analysis of the proposed rotation sensor with the earlier reported sensors is shown in Table I where the advantage of propose sensor can be appreciated. The above analysis shows that the design of a stable, linear wide dynamic range rotation sensor by considering the various other parameters is still in the nascent stage. Currently, the exploration of rotation sensor using the proposed configuration-I is under observation to improve its performance further. For the practical

implementation of the designed rotation/displacement sensor, commercially available stepper motor, spacer and other circuitry would be utilized.

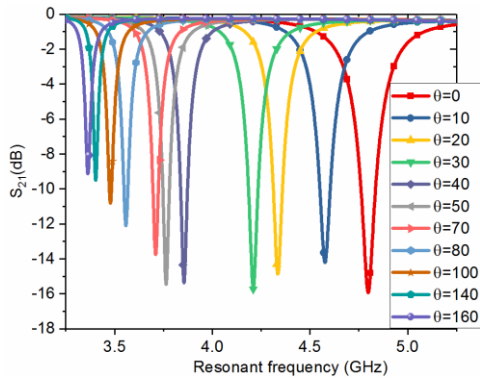


Figure 10. Plot of S21 for wide range of angular rotation.

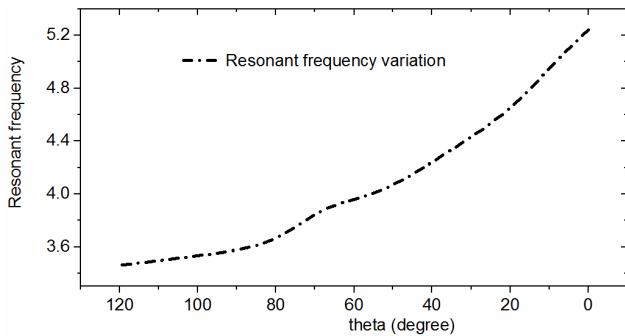


Figure 11. Graphical relation between resonant frequency and rotation angle ( $\Theta$ )

Table I: Performance Comparison of various rotation sensors

Sensors	Operational BW	Dynamic range	parameter	Sensitivity	structure
[11]	0.35 GHz	180 <sup>0</sup>	$\Delta f_r$	2.5 MHz/ <sup>0</sup>	U-shaped resonator
[10]	0.42 GHz	40 <sup>0</sup>	$\Delta f_r$	26 MHz/ <sup>0</sup>	NSRR
[5]	0.5 GHz @ 1mm	90 <sup>0</sup>	$\Delta S_{21}$	0.26 dB/ <sup>0</sup>	ELC
[9]	-	6 <sup>0</sup>	$\Delta S_{21}$	1 dB/ <sup>0</sup>	Horn SRR
proposed	2 GHz	120 <sup>0</sup>	$\Delta f_r$	19/ <sup>0</sup>	Separated ring of DSRR

#### 4. Conclusion

To the authors best knowledge, the vertically separated rings of the DSRR has been employed for the first time to

realize the contactless rotation/angular displacement sensor. The proposed sensor configuration has potential to realize the planar microwave rotation sensor with better dynamic range, linearity and sensitivity over the wide operational bandwidth. The analytical formulation, linearity range and resolution improvement with viable means of its practical implementation is under consideration.

#### 6. Acknowledgements

Author would like to thank the Mr. Abhishek Sharma, PhD Scholar, IIT Kanpur for his valuable suggestion and discussion.

#### 7. References

1. T. Chen, S. Li, and H. Sun, "Metamaterials application in sensing," *Sensors*, vol. 12, no. 3, pp. 2742–2765, 2012.
2. W. Withayachumnankul, K. Jaruwongrungrsee, A. Tuantranont, C. Fumeaux, and D. Abbott, "Metamaterial-based microfluidic sensor for dielectric characterization," *Sensors Actuat. A, Phys.*, vol. 189, pp. 233–237, Jan. 2013.
3. W. Withayachumnankul, K. Jaruwongrungrsee, C. Fumeaux, and D. Abbott, "Metamaterial-Inspired multichannel thin-film sensor," *IEEE Sensors J.*, vol. 12, no. 5, pp. 1455–1458, May 2012.
4. L. F. Chen, C. K. Ong, C. P. Neo, V. V. Varadan, and V. K. Varadan, *Microwave Electronics Measurement and Materials Characterization*. New York, NY, USA: Wiley, 2004, pp. 208–238.
5. J. Naqui and F. Marti'n, "Transmission lines loaded with bisymmetric resonators and their application to angular displacement and velocity sensors," *IEEE Trans Microw. Theory Tech.*, vol. 61, no. 12, pp. 4700–4713, 2013.
6. C. Herrojo, J. Mata-Contreras, F. Paredes and F. Marti'n, "Microwave encoders for chipless RFID and angular velocity sensors based on s-shaped split ring resonators," *IEEE Sensors J.*, vol. 17, no. 15, pp. 4805–4813, 2017.
7. J. Mata-Contreras, C. Herrojo and F. Marti'n, "Application of split ring resonator (SRR) loaded transmission lines to the design of angular displacement and velocity sensors for space applications", *IEEE Trans Microw. Theory Tech.*, vol. 65, pp. 4450–4460, 2017.
8. V. Sipal, A. Z. Narbudowicz and M. J. Ammann, "Contactless measurement of angular velocity using circularly polarized antennas," *IEEE Sensors J.*, vol. 15, no. 6, pp. 3459–3466, 2015.
9. A. K. Horestani, D. Abbott and C. Fumeaux, "Rotation sensor based on horn-shaped split ring resonator," *IEEE Sensors J.*, vol. 13, no. 8, pp. 3014–3015, 2013.
10. A. Maleki Gargari *et al.*, "A wireless metamaterial-inspired passive rotation sensor with submilliradian resolution," *IEEE Sensors J.*, vol. 18, pp. 4482–4490, 2018.
11. A. Ebrahimi, W. Withayachumnankul, S. F. Al-Sarawi and D. Abbott, "Metamaterial-Inspired rotation sensor with wide dynamic range," *IEEE Sensors J.*, vol. 14, no. 8, pp. 2609–2614, 2014.